Sae2 promotes DNA damage resistance by removing the Mre11–Rad50–Xrs2 complex from DNA and attenuating Rad53 signaling

Huan Chen[a,b], Roberto A. Donnianni[a,1], Naofumi Handa[c,1], Sarah K. Deng[a,1], Julyun Oh[a,b], Leonid A. Timashev[a], Stephen C. Kowalczykowski[c,2], and Lorraine S. Symington[a,2]

[a]Department of Microbiology & Immunology, Columbia University Medical Center, New York, NY 10032; [b]Department of Biological Sciences, Columbia University, New York, NY 10016; and [c]Department of Microbiology & Molecular Genetics and Department of Molecular and Cellular Biology, University of California, Davis, CA 95616

Contributed by Stephen C. Kowalczykowski, February 18, 2015 (sent for review January 7, 2015; reviewed by David O. Ferguson and John H. J. Petrini)

The Mre11–Rad50–Xrs2/NBS1 (MRX/N) nuclease/ATPase complex plays structural and catalytic roles in the repair of DNA double-strand breaks (DSBs) and is the DNA damage sensor for Tel1/ATM kinase activation. *Saccharomyces cerevisiae* Sae2 can function with MRX to initiate 5′-3′ end resection and also plays an important role in attenuation of DNA damage signaling. Here we describe a class of *mre11* alleles that suppresses the DNA damage sensitivity of *sae2*Δ cells by accelerating turnover of Mre11 at DNA ends, shutting off the DNA damage checkpoint and allowing cell cycle progression. The *mre11* alleles do not suppress the end resection or hairpin-opening defects of the *sae2*Δ mutant, indicating that these functions of Sae2 are not responsible for DNA damage resistance. The purified $M^{P110L}RX$ complex shows reduced binding to single- and double-stranded DNA in vitro relative to wild-type MRX, consistent with the increased turnover of Mre11 from damaged sites in vivo. Furthermore, overproduction of Mre11 causes DNA damage sensitivity only in the absence of Sae2. Together, these data suggest that it is the failure to remove Mre11 from DNA ends and attenuate Rad53 kinase signaling that causes hypersensitivity of *sae2*Δ cells to clastogens.

DNA repair | Mre11 | Sae2 | DNA damage checkpoint

Maintenance of genome integrity relies on the evolutionarily conserved DNA damage response (DDR), a coordinated network involving damage recognition, signal transduction, cell cycle regulation, and DNA repair (1). The DDR is activated by DSBs and by single-stranded DNA (ssDNA) that is formed by 5′-3′ resection of DSBs or when DNA replication is perturbed. The Tel1 and Mec1 protein kinases, orthologs of human ATM and ATR, respectively, initiate DNA damage signaling in *Saccharomyces cerevisiae* (2). Tel1/ATM is activated by Mre11–Rad50–Xrs2/NBS1 (MRX/N) nuclease/ATPase bound to DSB ends, whereas Mec1/ATR (in association with Ddc2/ATRIP) responds to replication protein A (RPA)-coated ssDNA (3, 4). Once activated by damaged DNA, Tel1 and Mec1 can directly phosphorylate key repair proteins, and they propagate their checkpoint signals through the Rad53 and Chk1 effector kinases (vertebrate Chk2 and Chk1, respectively) to halt the cell cycle and induce transcription of target genes (1).

In addition to its role as a sensor, the MRX/N complex plays scaffolding and catalytic roles in the repair of DSBs in eukaryotic cells (5). Mre11 functions as a dimer and exhibits DNA binding, as well as Mn^{2+}-dependent 3′-5′ dsDNA exonuclease and ssDNA endonuclease activities (6). The exonuclease activity of Mre11 is of the opposite polarity to that predicted for generation of 3′ overhangs although Mre11 is important for 5′-3′ end resection. A solution to this paradox has come from recent studies supporting a model whereby Sae2 (Ctp1 in *Schizosaccharomyces pombe* and CtIP in vertebrate cells) activates the Mre11 endonuclease to incise the 5′ strand at a distance from the end, followed by resection from the nick in a bidirectional manner using the Mre11 3′-5′ and Exo1 5′-3′ exonucleases (7–11). In addition, MRX can recruit Exo1 or Sgs1 helicase and Dna2 nuclease to ends to initiate resection of endonuclease-induced DSBs independently of the Mre11 nuclease activity and Sae2 (12–16). Exo1 and Sgs1-Dna2 act redundantly to produce long tracts of ssDNA (17).

Loss of any component of the MRX complex in *S. cerevisiae* results in sensitivity to DNA damaging agents, elimination of Tel1 signaling, short telomeres, defective nonhomologous end joining (NHEJ), and inability to process hairpin-capped ends or meiosis-specific DSBs that form via covalent attachment of the Spo11 topoisomerase-like protein to the 5′ terminated strands (18). Although elimination of the Mre11 nuclease activity (e.g., *mre11-H125N* mutation) or Sae2 also results in failure to process meiosis-specific DSBs and hairpins (19–22), the cells are more resistant to DNA damaging agents than Mre11-deficient cells (23). A class of hypomorphic *rad50* mutants, referred to as *rad50S*, is phenotypically similar to *mre11-H125N* and *sae2*Δ mutants (24). The *sae2*Δ mutant shows a delay in the initiation of resection at endonuclease-induced DSBs, but ultimately gene conversion repair occurs with normal frequency raising the question of why the *sae2*Δ mutant exhibits sensitivity to DNA damaging agents. One possibility is that DNA damaging agents, such as ionizing radiation, create ends that are not easily processed by Exo1 or Dna2 and require clipping by MRX and Sae2. Alternatively, the DNA damage sensitivity might be unrelated to the resection function of Mre11 nuclease and Sae2. Sae2 also plays an important role in modulating the

Significance

Chromosomal double-strand breaks (DSBs) are cytotoxic forms of DNA damage that must be accurately repaired to maintain genome integrity. The conserved Mre11–Rad50–Xrs2/NBS1 nuclease/ATPase complex plays an important role in repair by functioning as a damage sensor and by regulation of DNA end processing to ensure repair by the most appropriate mechanism. Yeast Sae2 is known to function with Mre11 to process DNA ends, but its precise role is poorly understood. Here we show that it is the failure to remove Mre11 from DNA ends, leading to persistent DNA damage signaling and cell cycle arrest, that causes sensitivity of Sae2-deficient cells to DNA damaging agents.

Author contributions: H.C., R.A.D., N.H., S.K.D., S.C.K., and L.S.S. designed research; H.C., R.A.D., N.H., S.K.D., J.O., and L.A.T. performed research; H.C., N.H., L.A.T., S.C.K., and L.S.S. contributed new reagents/analytic tools; H.C., R.A.D., N.H., S.K.D., J.O., L.A.T., S.C.K., and L.S.S. analyzed data; and H.C., S.C.K., and L.S.S. wrote the paper.

Reviewers: D.O.F., The University of Michigan Medical School; and J.H.J.P., Memorial Sloan–Kettering Cancer Center.

The authors declare no conflict of interest.

[1]R.A.D., N.H., and S.K.D. contributed equally to this work.

[2]To whom correspondence may be addressed. Email: lss5@columbia.edu or sckowalczykowski@ucdavis.edu.

This article contains supporting information online at www.pnas.org/lookup/suppl/doi:10.1073/pnas.1503331112/-/DCSupplemental.

checkpoint state, monitored by Rad53 phosphorylation (Rad53-P) (25). The DNA damage checkpoint is activated by induction of an unrepairable DSB and can be eventually turned off, allowing cells to divide through a process referred to as adaptation (26). *sae2*Δ mutants are defective for adaptation because they retain Rad53-P and fail to divide (25). This checkpoint alteration may result from a persistent signal generated by MRX accumulation at the DNA damaged site.

Here, we sought to determine whether the DNA damage sensitivity of the *sae2*Δ mutant is due to failure to process ends or inability to attenuate the DNA damage checkpoint by isolating suppressors of the *sae2*Δ mutant. We describe a class of *mre11* alleles that suppress the DNA damage sensitivity of the *sae2*Δ mutant by removing Mre11 from break ends and shutting off the DNA damage checkpoint without altering DNA end processing.

Results

Identification of *mre11* Alleles That Suppress *sae2*Δ DNA Damage Sensitivity. We reasoned that if the main function of Sae2 is to activate the Mre11 nuclease, then it might be possible to isolate gain-of-function *mre11* alleles that bypass the requirement for Sae2. A plasmid containing *MRE11* was randomly mutagenized by passage through an *Escherichia coli* mutator strain and the pool of plasmids used to transform an *mre11*Δ *sae2*Δ mutant. The *mre11*Δ and *sae2*Δ mutations confer sensitivity to camptothecin (CPT); thus, we anticipated an *mre11* gain-of-function allele to complement *mre11*Δ and to suppress the sensitivity caused by loss of Sae2. One plasmid was recovered with a single nucleotide change resulting in substitution of Mre11 Pro110 with Leu. The *MRE11* locus of a *sae2*Δ strain was replaced with the *mre11-P110L* allele, and the resulting strain showed >100-fold higher CPT and methylmethane sulfonate (MMS) resistance compared with the *sae2*Δ mutant (Fig. 1*A*). In addition, *mre11-P110L* suppressed the CPT and MMS sensitivity of *rad50S* cells (Fig. 1*A*). The *mre11-P110L* mutant exhibited no obvious sensitivity to DNA damaging agents.

The *MRE11* mutagenesis was repeated by a PCR method, resulting in recovery of five alleles that suppressed the CPT and MMS sensitivity of *mre11*Δ *sae2*Δ cells. Of these, one was again due to substitution of Pro110 with Leu and the others had substitutions of residues His37, Gln70, Thr74, or Glu101 (Fig. 1*B*). The mutations are of nonconserved residues and are not in well-defined structural motifs of Mre11. Analysis by protein blotting revealed that all of the mutants expressed normal levels of Mre11; however, the Mre11^{P110L} and Mre11^{E101G} proteins both showed slightly faster mobility than Mre11 (Fig. S1*A*). The structure of the *S. pombe* Mre11–Nbs1 complex shows Mre11 Glu101 and Pro110 are within the eukaryotic-specific "latching loop" of Mre11 and Pro110 is a site of direct interaction with Nbs1 (Fig. S1*B*) (27). Several mutations in human *MRE11* that cause ataxia telangiectasia or Nijmegen breakage-like syndromes are located within the latching loop and result in a reduced affinity for NBS1 (27). Although Mre11^{P110L} retains interaction with Xrs2, we consistently recovered less Xrs2 in immunoprecipitates compared with Mre11 (Fig. 1*C*).

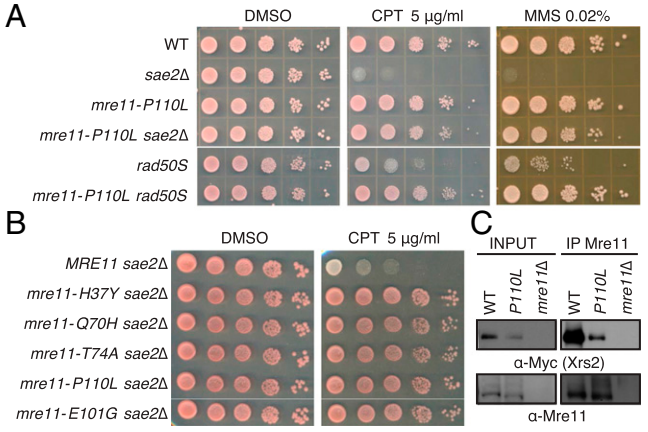

Fig. 1. Identification of *mre11* alleles that suppress *sae2*Δ DNA damage sensitivity. (*A*) Tenfold serial dilutions of log-phase cultures of the indicated strains were spotted onto SC medium with DMSO alone or DMSO + 5 μg/mL CPT, or YPD medium with 0.02% MMS. (*B*) Tenfold serial dilutions of log-phase *mre11*Δ *sae2*Δ cells expressing *MRE11* or *mre11* alleles from pRS416 were spotted onto SC-URA medium with DMSO alone or DMSO + 5 μg/mL CPT. (*C*) Coimmunoprecipitation of Myc-tagged Xrs2 by Mre11 antibody in wild type, *mre11-P110L*, and *mre11*Δ cells. WT refers to wild-type cells.

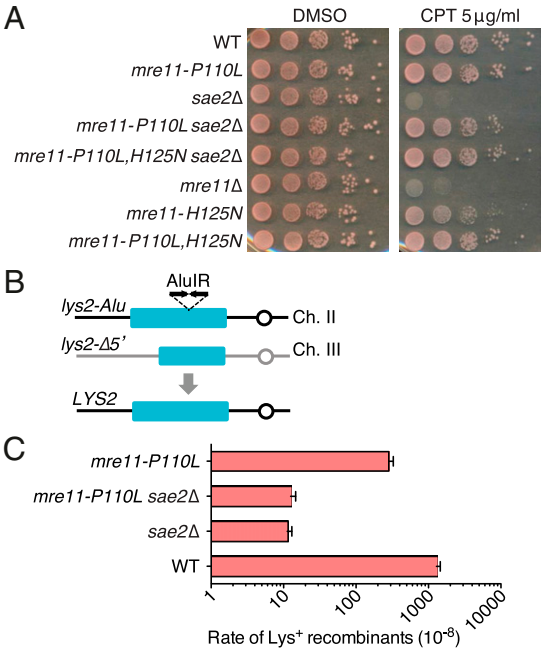

Fig. 2. The *mre11* alleles do not activate the Mre11 nuclease independently of Sae2. (*A*) Tenfold serial dilutions of log phase *mre11*Δ or *mre11*Δ *sae2*Δ cells expressing *MRE11*, *mre11-P110L*, *mre11-H125N*, or *mre11-P110L, H125N* from a plasmid were spotted onto SC-URA medium with DMSO alone or DMSO + 5 μg/mL CPT. (*B*) Schematic representation of the *lys2-AluIR* and *lys2*-Δ5′ ectopic recombination reporter. (*C*) Graph showing the rate of Lys$^+$ recombinants in different strains determined by fluctuation analysis. The mean values from three independent trials are plotted, and error bars show SD.

Suppression of *sae2*Δ by *mre11-P110L* Is Independent of the Mre11 Nuclease Activity. Our screen was based on the premise that Sae2 activates the Mre11 nuclease; if so, the suppressive effect of *mre11-P110L* should be eliminated by a point mutation in one of the Mre11 phosphoesterase motifs (18). The His125 to Asn substitution was generated by site-directed mutagenesis of the plasmid harboring the *mre11-P110L* allele. The resulting plasmid was used to transform *mre11*Δ and *mre11*Δ *sae2*Δ mutants, and independent transformants were tested for CPT resistance. Surprisingly, the *mre11-P110L, H125N* allele showed equivalent suppression of the *sae2*Δ CPT sensitivity as the *mre11-P110L* allele, indicating that the suppression is independent of Mre11 nuclease activity (Fig. 2*A*). Indeed, the *mre11-P110L, H125N* allele suppressed the DNA damage sensitivity of *mre11*Δ cells to a greater extent than *mre11-H125N*, indicating that *mre11-P110L* suppresses the DNA damage sensitivity associated with loss of the Mre11 nuclease.

***mre11-P110L* Does Not Suppress the Hairpin-Opening or Resection Defect of the *sae2*Δ Mutant.** To determine whether *mre11-P110L* bypasses the requirement for Sae2 in hairpin resolution, we

generated *mre11-P110L* derivatives of haploid strains with the *lys2-AluIR* and *lys2-Δ5′* ectopic recombination reporter (Fig. 2*B*). The inverted Alu elements stimulate ectopic recombination by ~1,000-fold relative to a strain with a direct repeat of Alu elements inserted at the same site in *lys2*, and this stimulation largely depends on the MRX complex, the Mre11 nuclease, and Sae2 (19). The inverted repeats are thought to extrude to form a hairpin or cruciform that is cleaved by an unknown nuclease to form a hairpin-capped end, which is then opened by MRX-Sae2 and stimulates recombination to generate a functional *LYS2* gene. The *mre11-P110L* mutation failed to suppress the hairpin resolution defect conferred by *sae2*Δ, indicating that it does not function by activating the Mre11 nuclease independently of Sae2 (Fig. 2*C*). All of the *mre11* alleles were tested by a semiquantitative plating assay, but none of them restored hairpin opening to the *sae2*Δ mutant (Fig. S2*A*). In addition, the *mre11-P110L, H125N* allele did not complement the hairpin-opening defect of the *mre11*Δ mutant (Fig. S2*A*). Notably, the *mre11-P110L* mutant exhibited a small, but significant, decrease in the generation of Lys^+ recombinants ($P < 0.0001$), indicating that hairpin cleavage or HR repair is not fully functional. The *mre11-P110L* mutation was unable to restore sporulation to the *sae2*Δ mutant, suggesting it does not suppress the *sae2*Δ defect in Spo11 removal (Fig. S2*B*).

Because removal of Ku suppresses the CPT sensitivity and 5′-3′ resection defects of the *sae2*Δ mutant in an Exo1-dependent manner (15, 23, 28), we considered the possibility that *mre11-P110L* allows greater access of Exo1 to ends. If this were the case, the suppression of *sae2*Δ by *mre11-P110L* would be *EXO1* dependent. Although the *exo1*Δ mutation reduced the CPT and MMS resistance of the *mre11-P110L sae2*Δ strain by approximately 10-fold, the triple mutant was considerably more resistant than the *exo1*Δ *sae2*Δ double mutant, indicating that the suppression is largely independent of *EXO1* (Fig. 3*A*). We could not test whether *mre11-P110L* activates the Sgs1-Dna2 resection mechanism because of the lethality caused by combining *sae2*Δ and *sgs1*Δ mutations, which was not suppressed by *mre11-P110L* (Fig. S3*A*). To determine whether *mre11-P110L* and elimination of *yku70*Δ are additive in their suppression of *sae2*Δ, the CPT and MMS sensitivities of the double and triple mutants were compared. The *mre11-P110L sae2*Δ strain was more resistant to CPT and MMS than *sae2*Δ *yku70*Δ, and no further suppression was observed for the triple mutant; instead, the triple mutant showed the same CPT sensitivity as the *mre11-P110L sae2*Δ double mutant, but was more resistant to MMS than the *sae2*Δ *yku70*Δ mutant (Fig. 3*A*). Notably, *mre11-P110L* is effective in suppression of the CPT and MMS sensitivities of the *sae2*Δ mutant, whereas *yku70*Δ suppresses the CPT but not the MMS sensitivity of the *sae2*Δ mutant.

To test whether *mre11-P110L* suppresses the delayed resection initiation observed in *sae2*Δ cells, we measured the efficiency of single-strand annealing (SSA) between partial *leu2* gene repeats located 4.6 kb apart on chromosome III by Southern blot analysis (Fig. 3*B*) (29). The HO endonuclease-induced DSB is formed 30 min after expression of *HO* from the P_{GAL1} promoter, and, after sufficient resection to expose the flanking homology, the *leu2* sequences anneal to form a deletion product of 8 kb. The *sae2*Δ mutant exhibited a 30- to 60-min delay in formation of the SSA product relative to wild type, which was unchanged by *mre11-P110L* (Fig. 3*C*). End resection that proceeds beyond the flanking KpnI sites results in disappearance of the HO-cut fragments and appearance of a high molecular weight intermediate. Disappearance of the HO-cut fragments and generation of resection intermediates were delayed in the *sae2*Δ mutant, and this phenotype was also unaffected by the *mre11-P110L* mutation (Fig. S3*B*).

To test whether *mre11-P110L* has any affect on homologous recombination in the *sae2*Δ background, we monitored repair of the HO-induced DSB at the *MATα* locus by conversion to *MAT***a** (Fig. S3*C*). All of the strains showed the same efficiency of gene conversion repair. Together, these results show that the *mre11-P110L* mutant exhibits normal resection and HR repair and does not restore nuclease activity to the MRX complex in the absence of Sae2.

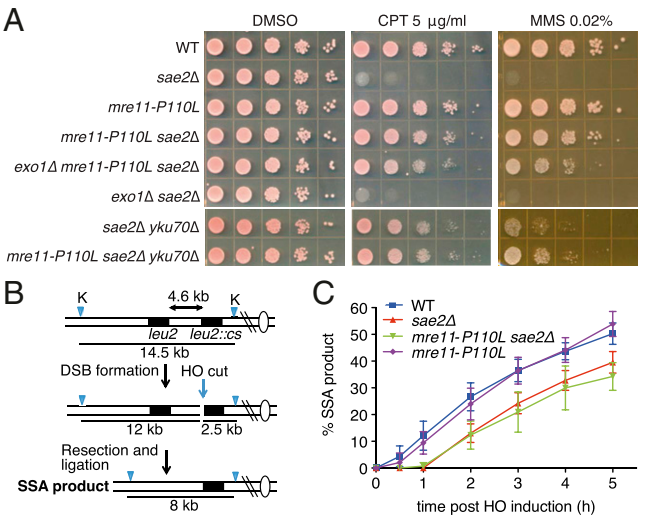

Fig. 3. Suppression of *sae2*Δ by *mre11-P110L* is independent of *EXO1* and does not restore end resection. (*A*) Tenfold serial dilutions of log-phase cultures of the indicated strains were spotted onto SC medium with DMSO alone or DMSO + 5 μg/mL CPT, or YPD medium with 0.02% MMS. (*B*) Schematic representation of the SSA assay system with two partial *leu2* repeats located 4.6 kb apart on chromosome III. The second copy of *leu2* harbors an HO endonuclease cut site. (*C*) Plot showing the ratio of SSA product among the total DNA in each lane at different time points after HO induction. The mean values from three independent trials are plotted, and error bars show SD.

***mre11-P110L* Bypasses the Checkpoint and Cell Cycle Progression Defects of *sae2*Δ Cells.** Because *mre11-P110L* failed to rescue the resection and hairpin resolution defects of the *sae2*Δ mutant, the increased DNA damage resistance could be the result of checkpoint inactivation. To test this, we analyzed Rad53-P in wild-type, *mre11-P110L*, *sae2*Δ, and *mre11-P110L sae2*Δ strains following an acute treatment with MMS (0.015% for 1 h). Extracts prepared from cells collected after MMS treatment were analyzed by Western blot using anti-Rad53 antibodies. Rad53-P was detected as an electrophoretic mobility shift in response to MMS in all of the strains. The phosphorylated form of Rad53 was present for up to 1 h following MMS treatment in wild-type cells, and then Rad53 migrated as the unmodified form at 3 h (Fig. 4*A*). In the *sae2*Δ mutant, Rad53 remained phosphorylated for 3 h; in contrast, Rad53 was deactivated at 3 h in the *mre11-P110L sae2*Δ mutant. Rad53-P, in response to MMS, was analyzed for all of the *mre11* mutations and all suppressed the *sae2*Δ defect (Fig. S4*A*).

At the time of release from a 2-h MMS treatment (0.02%), cells from all strains were arrested in S phase (Fig. 4*B*). Wild-type and *mre11-P110L* cells progressed to G_2/M 1 h after removal of MMS from the culture, initiated division at 2 h, and by 4 h, the FACS profile was similar to untreated cells. By contrast, *sae2*Δ cells remained in S phase for 2 h after removal of MMS from the culture and had not resumed division at 4 h, consistent with impaired DNA replication (30). The *mre11-P110L* mutation partially suppressed the S-phase progression defect caused by *sae2*Δ, and cells resumed division 3 h after MMS treatment. In agreement with the FACS profile, the suppression of *sae2*Δ by *mre11-P110L* was also seen by the plating efficiency of cells following acute MMS exposure (Fig. 4*C*).

Because *mre11-P110L* suppressed the *sae2*Δ checkpoint shut off defect, we tested whether elimination of Tel1 could also suppress *sae2*Δ. We found no suppression of the *sae2*Δ DNA damage

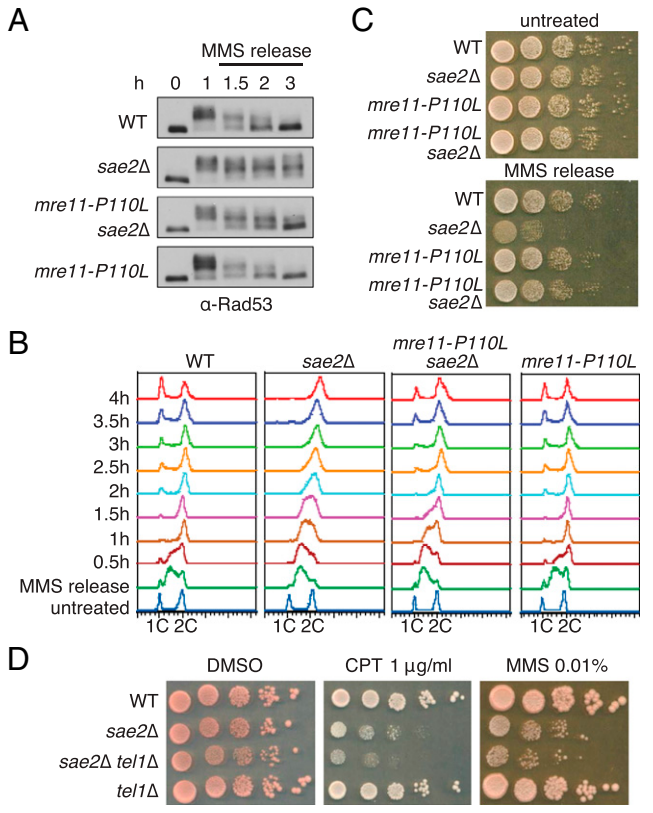

Fig. 4. *mre11-P110L* suppresses the DNA damage checkpoint recovery defect caused by *sae2*Δ. (*A*) Western blot analysis showing Rad53-P and dephosphorylation in response to MMS. Log-phase growing cells ($t = 0$) from indicated strains were treated with 0.015% MMS for 1 h and released into fresh YPD ($t = 1$ h). Protein samples from different time points before and after MMS treatment were analyzed by using anti-Rad53 antibodies. (*B*) FACS profiles of DNA content from indicated strains in response to 0.02% MMS for 2 h and following release into YPD. Cell samples were taken before MMS treatment and at the indicated time points after MMS release for FACS analysis. (*C*) Tenfold serial dilutions of MMS-treated cells in *B* were spotted onto YPD solid medium to monitor colony formation with untreated cells from the same starting cultures spotted as controls. (*D*) Tenfold serial dilutions of log-phase cultures of the indicated strains were spotted onto SC medium with DMSO alone or DMSO + 1 μg/mL CPT, or YPD medium with 0.01% MMS.

sensitivity by *tel1*Δ; on the contrary, the *sae2*Δ *tel1*Δ double mutant exhibited higher sensitivity to low doses of CPT and MMS than the *sae2*Δ single mutant (Fig. 4*D*). A previous study had shown that *sae2*Δ suppresses the MMS sensitivity of the *mec1*Δ mutant by activating MRX-Tel1–mediated checkpoint signaling (31). If *mre11-P110L* acted by dampening the MRX-Tel1 pathway, we would predict it to sensitize the *mec1*Δ *sae2*Δ mutant; instead, the *mec1*Δ *mre11-P110L sae2*Δ strain showed an equivalent MMS sensitivity to the *mec1*Δ *sae2*Δ strain (Fig. S4*B*).

Turnover of Mre11 at DNA Ends Is Altered by the P110L Mutation. Previous studies have shown that Mre11 is retained at DSBs for longer in the absence of Sae2 or the Mre11 nuclease (25, 28, 32). Furthermore, overexpression of *SAE2* results in faster turnover of Mre11 at DNA ends and correlates with reduced Rad53-P (25). Thus, one possible mechanism for the *mre11-P110L* attenuation of Rad53-P would be by accelerated turnover of Mre11 at DNA ends. We tagged the C termini of $Mre11^{P110L}$ and $Mre11^{H37Y}$ with YFP to monitor the recruitment and turnover of Mre11 complexes at DSBs by fluorescence microscopy (Fig. 5*A*). Cells were exposed to 40-Gy γ-irradiation, and foci were counted at 0.5, 1, 2, and 3 h later. As reported previously, ~50% of cells formed Mre11 foci in response to irradiation and the number of cells with foci declined to 22% after 3 h. By contrast, 90% of *sae2*Δ cells exhibited Mre11 foci 0.5 h after irradiation and 60% of cells retained Mre11 foci 3 h later. The lower number of cells with Mre11 foci 30 min after irradiation in wild type compared with *sae2*Δ cells is most likely due to more rapid turnover of Mre11 when Sae2 is present. $Mre11^{P110L}$-YFP and $Mre11^{H37Y}$-YFP both dissociated from IR-induced DSBs faster than Mre11-YFP in the *sae2*Δ background (Fig. 5*B*). $Mre11^{P110L}$-YFP and $Mre11^{H37Y}$-YFP showed similar kinetics to Mre11-YFP in *SAE2* cells. In agreement with the DNA damage sensitivity, *tel1*Δ failed to suppress the persistent Mre11-YFP foci in the *sae2*Δ mutant (Fig. S5*A*). To confirm these data, Mre11 association with sequences 1 kb away from an HO-induced DSB was measured by chromatin immunoprecipitation (ChIP). Mre11 was detected at higher levels adjacent to the DSB in *sae2*Δ cells compared with wild type, and dissociated more slowly (Fig. 5*C*). $Mre11^{P110L}$ was recruited with similar kinetics but dissociated from the DSB faster in *sae2*Δ cells than Mre11, consistent with the foci data. The ChIP assays were performed in a strain that is unable to repair the HO-induced DSB because the *HM* donors are deleted; thus, the increased turnover of $Mre11^{P110L}$ in the *sae2*Δ mutant is not a consequence of altered repair kinetics.

***mre11-P110L* Mutation Partially Suppresses the *sae2*Δ Hyper-NHEJ Phenotype.** The *sae2*Δ mutant exhibits an elevated NHEJ frequency (33), which could result from delayed resection and/or retention of MRX or Ku at ends. Because *mre11-P110L* does not suppress the end resection defect of *sae2*Δ, but suppresses retention of Mre11 at ends, we tested whether NHEJ repair of a chromosomal I-SceI–induced DSB is reduced in *mre11-P110L* derivatives. The end joining assay was designed with a 14-bp direct repeat flanking an inverted duplication of I-SceI cut sites to measure both NHEJ and microhomology-mediated end joining (MMEJ) repair (34). The *mre11-P110L* mutant showed the same frequency of NHEJ as the wild-type strain ($P = 0.57$); however, *mre11-P110L* significantly reduced NHEJ in the *sae2*Δ background ($P < 0.05$) (Fig. 5*D*). These data suggest retention of MRX at ends is responsible for increased NHEJ in *sae2*Δ cells.

The $M^{P110L}RX$ Complex Exhibits Reduced DNA Binding in Vitro. The increased turnover of $Mre11^{P110L}$ at DSBs could reflect reduced affinity of the mutant protein for DNA. To directly test this hypothesis, MRX and $M^{P110L}RX$ complexes were purified (Fig. S5*B*) and assayed for binding to single- or double-stranded DNA by electrophoretic mobility shift (Fig. 5*E*). The $M^{P110L}RX$ complex showed reduced binding to both DNA substrates in the presence of Mg^{2+} or Mn^{2+} (Fig. 5*F*). Consistent with reduced DNA binding, we detected weaker 3′-5′ exonuclease activity for the $M^{P110L}RX$ mutant complex compared with the wild-type MRX complex (Fig. S5*C*). Addition of ATP stimulated binding of both wild-type and mutant complexes, but $M^{P110L}RX$ still exhibited lower DNA binding than MRX (Fig. S5 *D* and *E*).

***MRE11* Gene Dosage Alters *sae2*Δ DNA Damage Sensitivity.** Our expectation when we isolated *mre11* alleles that complemented the *mre11*Δ mutation and suppressed the DNA damage sensitivity caused by *sae2*Δ was for a gain of function; however, the in vitro analysis suggests a loss of function. To assess dominance, diploids homozygous for *sae2*Δ and homozygous or heterozygous for *mre11-P110L* were generated. Diploids expressing one copy of *mre11-P110L* showed similar MMS resistance to haploid *sae2*Δ *mre11-P110L* cells, whereas *sae2*Δ/*sae2*Δ *MRE11*/*mre11-P110L* cells exhibited intermediate MMS resistance, indicating semi-dominance of *mre11-P110L* (Fig. 6*A*). Surprisingly, diploid cells homozygous for *sae2*Δ and *mre11-P110L* were more sensitive to MMS than *sae2*Δ/*sae2*Δ *mre11-P110L*/*mre11*Δ cells. Furthermore,

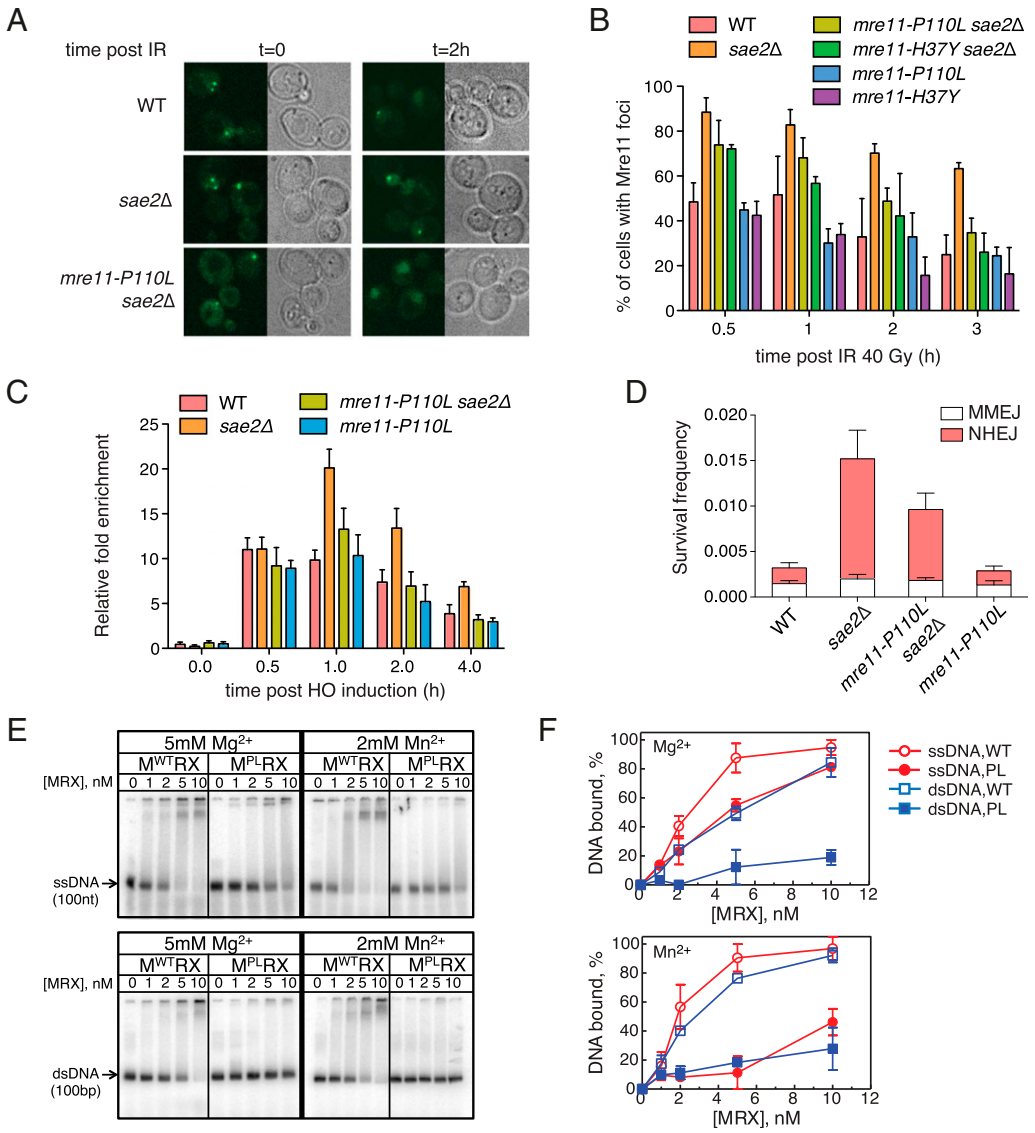

Fig. 5. Turnover of Mre11 proteins at DSB ends is altered by Mre11^{P110L}. (*A*) Epifluorescence microscopy showing DSB induced foci formation of Mre11-YFP or Mre11^{P110L}-YFP following IR (40 Gy). (*B*) Quantification of Mre11-YFP, Mre11^{P110L}-YFP, or Mre11^{H37Y}-YFP foci from indicated strains. The percentage of cells with one or more YFP foci at different time points after IR was quantitated. The mean values from three independent trials are plotted, and error bars show SD. (*C*) Graph showing Mre11 association with sequences 1 kb away from a nonrepairable HO-induced DSB at the *MAT* locus. Cell samples collected at the indicated time points after HO induction were analyzed. The mean values from three independent trials are plotted, and error bars show SD. (*D*) A chromosomal end-joining assay was used to measure NHEJ and MMEJ frequency from indicated strains, where repair by HR is unable to form survivors. The mean values from three independent trials are plotted, and error bars show SD. (*E*) DNA binding assay using purified yeast MRX or M^{P110L}RX complex in the presence of 5 mM Mg^{2+} or 2 mM Mn^{2+}. A 100-nt ssDNA substrate or 100-bp dsDNA substrate was used. (*F*) Quantification of the data shown in *E*. The mean values from two independent trials are plotted and error bars show SE.

*sae2*Δ homozygous diploids expressing only one *MRE11* allele were slightly more MMS resistant than cells expressing two copies. These data indicate that the level of Mre11 (wild type or mutant) modulates DNA damage sensitivity of *sae2*Δ cells.

Because the *sae2*Δ diploid is sensitive to *MRE11* gene dosage, we asked whether overexpression of *MRE11* would further sensitize *sae2*Δ haploid cells. We compared the CPT and MMS sensitivity of cells expressing *MRE11* from the natural promoter on a single-copy number plasmid (centromere [*CEN*]-containing vector) with cells expressing *MRE11* from a high-copy number (2μ) plasmid (Fig. 6*B*). Remarkably, overexpression of *MRE11* resulted in greater sensitivity to CPT and MMS only in the absence of *SAE2*, consistent with the notion that Sae2 actively removes Mre11 from break ends.

Discussion

Genetic and biochemical studies show that Sae2 functions with the MRX complex to initiate DNA end resection in yeast (8, 11, 35). The current model is for Sae2 to stimulate Mre11 endonucleolytic clipping of the 5′-terminated strand with the resulting nick acting as an entry site for bidirectional processing by the Mre11 and Exo1 exonucleases (7, 9–11). Consequently, loss of Sae2 or the Mre11 nuclease results in retention of Spo11 at meiotic DSBs and failure to resolve hairpin-capped ends (18). Resection of unblocked ends (e.g., those produced by endonucleases) can occur in the absence of Sae2 or the Mre11 nuclease activity via recruitment of Exo1 or Sgs1-Dna2 by the MRX complex (15, 35–37). Although *sae2*Δ and *mre11-H125N* mutants are equivalent in their inability to resolve Spo11 adducts and hairpin-capped ends, the *sae2*Δ

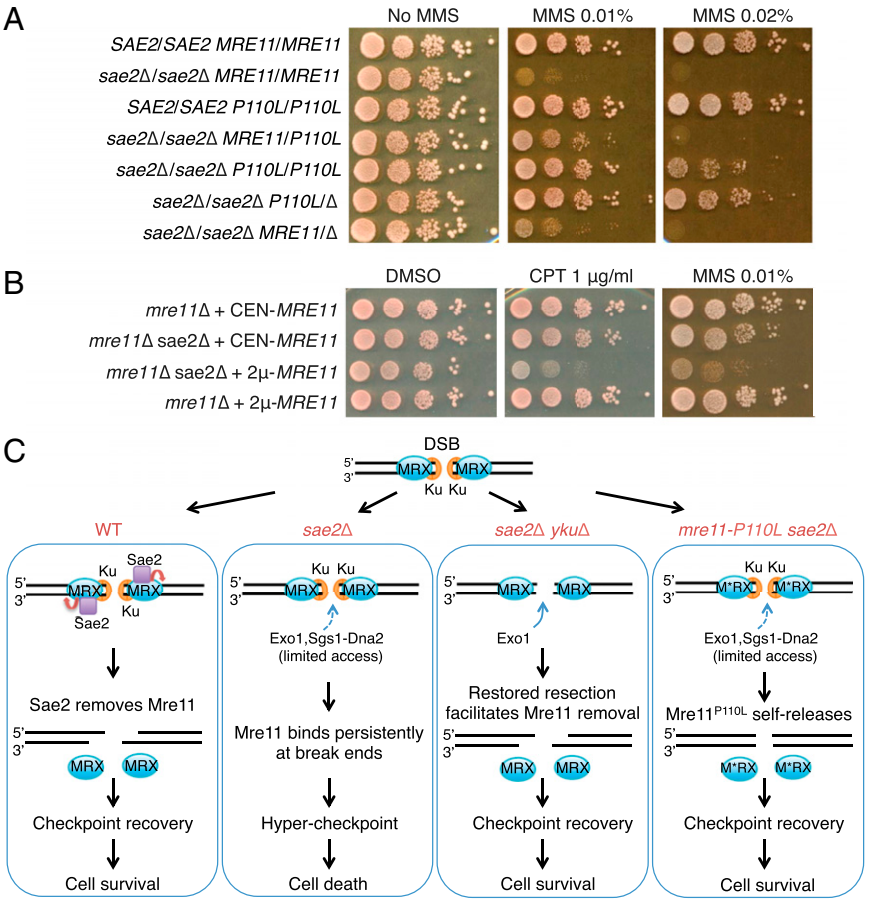

Fig. 6. Mre11 is toxic in the absence of Sae2. (*A*) Tenfold serial dilutions of log phase diploid cells with the indicated genotype were spotted onto YPD medium with no MMS, 0.01% MMS, or 0.02% MMS. (*B*) Tenfold serial dilutions of log phase *mre11*Δ or *mre11*Δ *sae2*Δ haploid cells expressing *MRE11* from a CEN or 2μ-based plasmid were spotted onto SC-URA medium containing DMSO alone, or DMSO + 1 μg/mL CPT, or YPD medium with 0.01% MMS. (*C*) Model showing resection-dependent and resection-independent suppression of *sae2*Δ DNA damage sensitivity by removing Mre11 from DSB ends and attenuating DNA damage checkpoint signaling.

phenotype is slightly more severe than observed for *mre11-H125N* with regards to sensitivity to DNA damaging agents and removal of Mre11 from DNA ends (23, 32). To gain insight into how Sae2 and the Mre11 nuclease cooperate to initiate end resection, we screened for *mre11* gain-of-function alleles that could bypass the DNA damage sensitivity conferred by the *sae2*Δ mutation. Here, we describe *mre11* alleles that suppress *sae2*Δ DNA damage sensitivity by promoting Mre11 dissociation and shutting off the DNA damage checkpoint, not by activation of end processing, indicating that the major function of Sae2 in the DNA damage response is to remove MRX complex from break ends (Fig. 6*C*).

None of the *mre11* mutations was able to suppress the hairpin resolution or sporulation defects of the *sae2*Δ mutant although all suppressed the DNA damage sensitivity by >100-fold. Further characterization of *mre11-P110L* showed that it is unable to suppress the subtle resection defect of the *sae2*Δ mutant, and that suppression of the *sae2*Δ CPT sensitivity is independent of the Mre11 nuclease activity and mostly Exo1 independent. By contrast, *yku70*Δ restores resection and resistance to DSB-inducing agents to the *sae2*Δ mutant in an Exo1-dependent manner, and *rad9*Δ suppresses the *sae2*Δ end resection defect by allowing access to Sgs1-Dna2 (15, 23, 38–41). Deletion of *DNL4* (encoding DNA ligase IV) does not suppress the DNA damage sensitivity of *sae2*Δ, *mre11-3*, and *cpt1*Δ mutants, indicating that the *yku70*Δ suppression is by allowing Exo1 access to ends and not by diverting ends from NHEJ to HR (23, 28, 38). From these data, we conclude that the end-processing function of Sae2 is not the only determinant for DNA damage tolerance and that another function of Sae2 must contribute.

Previous studies reported that Mre11 remains associated with DNA ends for longer in the *sae2*Δ mutant and correlates with hyperphosphorylation of Rad53 (25). Overexpression of *SAE2* reduces Mre11 association with DNA ends and prevents Rad53-P in response to DSBs (25). The effect of Sae2 on Rad53-P does not directly correlate with resection or repair efficiency because Rad53 remains phosphorylated in the *sae2*Δ mutant in response to an unrepairable DSB although resection occurs, and overexpression of *SAE2* does not increase end resection. All of the *mre11* alleles that suppress the DNA damage sensitivity of the *sae2*Δ mutant show normal activation of Rad53 in response to DNA damaging agents, but partially suppress the defect in Rad53 dephosphorylation. Rad53-P in response to DNA damage is primarily by Mec1 with Tel1 playing a minor role (42, 43); however, in the absence of Sae2/Ctp1, the Tel1 pathway is activated, presumably because of the delay to resection initiation and retention of MRX at DSBs (31, 44). *mre11-P110L* does not decrease MMS sensitivity of the *mec1*Δ *sae2*Δ mutant, and the *mec1*Δ *mre11-P110L* double mutant showed equivalent MMS sensitivity to *mec1*Δ, suggesting that Tel1 signaling is not affected by *mre11-P110L*.

In vitro, the $M^{P110L}RX$ complex displayed reduced binding to both ssDNA and dsDNA compared with MRX. The reduced binding to DNA was also evident in vivo: association of $Mre11^{P110L}$ at an HO-induced DSB was slightly lower than observed for Mre11. We do not know whether the foci and ChIP signals reflect binding to dsDNA ends or to ssDNA. The dosage dependence for suppression of the DNA damage sensitivity of *sae2*Δ could also be attributed to Mre11 DNA binding: diploids homozygous for *sae2*Δ and with two copies of *mre11-P110L* showed reduced DNA damage resistance compared with cells expressing only one copy of *mre11-P110L*. Furthermore, overexpression of *MRE11* further sensitized the *sae2*Δ mutant, but not *SAE2* cells. These subtle differences suggest *sae2*Δ DNA damage resistance is sensitive to the level of Mre11, and by impairing Mre11 DNA binding

via the P110L mutation, the DNA damage checkpoint is alleviated and resistance to DNA damage is restored to the *sae2*Δ mutant. Although we favor the hypothesis that persistently bound MRX in the *sae2*Δ mutant results in hyperactivation of the DNA damage checkpoint and cell cycle arrest, we cannot exclude the possibility that DNA-bound MRX prevents HR repair and multiple unrepaired lesions cause persistent Rad53 signaling. By this scenario, *mre11-P110L* suppresses *sae2*Δ by facilitating MRX removal of ends to make them accessible for Rad51 binding and subsequent repair; thus, relieving the checkpoint signal.

In summary, our findings support a model whereby the major function of Sae2 in response to DSB is to actively remove MRX from break ends after resection initiation, partially through activating Mre11 endonuclease. The absence of this function causes persistent checkpoint signaling and cell cycle arrest, leading to reduced survival (Fig. 6*C*). The *sae2*Δ defect can be suppressed by elimination of Ku to allow access of Exo1, which activates resection and facilitates Mre11 dissociation (45). More importantly, it can also be suppressed in a resection independent manner via reduced DNA binding by Mre11 allowing self release; thus, attenuating checkpoint signaling and restoration of DNA damage resistance. Given that the *sae2*Δ mutant is considerably more sensitive to DNA damaging agents than the *mre11-H125N* mutant, Sae2 must be doing more than activation of the Mre11 nuclease. Recombinant Sae2 is also reported to have an intrinsic endonuclease activity (46). However, overexpression of *SAE2* does not increase end resection but reduces Mre11 association with DNA ends and prevents Rad53-P in response to DSBs (25), suggesting a nuclease independent function of Sae2 exists to remove Mre11 from break ends.

Experimental Procedures

Media, Growth Conditions, and Yeast Strains. Rich medium (yeast extract–peptone–dextrose, YPD), synthetic complete (SC) medium, and genetic methods were as described (47). CPT or MMS was added to SC or YPD medium, respectively, at the indicated concentrations. For survival assays, serial dilutions of log-phase cultures were spotted on plates and incubated for 2–3 d at 30 °C.

The yeast strains used are listed in Table S1. W303 derivatives were constructed by crossing isogenic strains present in our laboratory collection to produce haploid progeny of the indicated genotypes. For non-W303 strains, one-step gene replacement with PCR products was used to construct desired mutations. The *mre11-P110L* mutant was made by one-step gene replacement of an *mre11*::*URA3* strain with PCR fragment containing the *mre11-P110L* ORF and 500-bp upstream and downstream homologous sequence, selecting for 5-fluoroorotic acid resistance. A *NatMX* cassette flanked by 50-bp homologies to yeast genomic sequences was amplified from pAG25 and inserted into the 3′ UTR of the *mre11-P110L* strain, 266 bp downstream of the stop codon. The *mre11-P110L-YFP* and *mre11-H37Y-YFP* strains were made by two-step gene targeting of the *MRE11-YFP* strain (32).

Genetic Screens for *mre11* Mutations That Suppress *sae2*Δ. In the first screen, pRS416-*MRE11* was propagated in XL1-Red mutator *E. coli* cells (Agilent Technologies) for 15–30 generations, and purified plasmid DNA was used to transform *mre11*Δ *sae2*Δ cells. Transformants (3,400 total) were tested for suppression of the *sae2*Δ CPT sensitivity. Potential clones were recovered from yeast, amplified in *E. coli*, rescreened, and then subjected to DNA sequencing to identify the responsible mutations. In the second screen, the N-terminal region (−132 bp to 882 bp) of the *MRE11* ORF in pRS416-*MRE11* was randomly mutagenized by using GeneMorph II EZClone Domain Mutagenesis Kit (Agilent Technologies), transformed into *mre11*Δ *sae2*Δ cells and transformants were directly replica plated onto medium containing 5 μg/mL CPT. Survivors were further validated and then sequenced to identify the mutations. For plasmids containing more than one mutation, each was individually created by site-directed mutagenesis of pRS416-*MRE11* by using QuikChange Lightning Multi Site-Directed Mutagenesis Kit (Agilent Technologies).

In Vivo Hairpin Opening, SSA, and Mating-Type Switching Assays. Recombination rates were derived from the median Lys^+ recombination frequency determined from eight isolates of each strain as described (19). Three trials were performed, and the mean recombination rate was calculated. The SSA and mating-type switching assays were performed as described (29, 35).

Chromosomal End Joining Assay. The chromosomal end-joining substrate was constructed similarly to the one described except with 14-bp direct repeats flanking the inverted I-SceI cuts sites; the end joining assay was performed as described (34).

Epifluorescence Microscopy. Cells were grown in liquid SC medium at 25 °C to midlog phase, treated with 40 Gy (Gammacell-220 irradiator containing ^{60}Co), and processed for epifluorescence microscopy 0.5, 1, 2, and 3 h after IR. A spinning-disk confocal (CSU10; Yokagawa) inverted microscope (Eclipse Ti; Nikon) with a Hamamatsu EM-CCD camera, and a 60× 1.4 N.A. objective was used for image acquisition. In each field of cells, 15 images were obtained at 0.4-μm intervals along the *z* axis to allow inspection of all focal planes of cells. Image acquisition time for lightfield and YFP were 150 ms and 500 ms, respectively. Images were analyzed by using Micromanager, and cells with one or more foci were scored with maximum-intensity projection.

Coimmuniprecipitation and ChIP Assays. Coimmuniprecipitation was performed as described by using Mre11 polyclonal antibodies from rabbit serum (48). Mre11 and Xrs2-myc were detected by Western blot using Mre11 and myc (Abcam) antibodies, respectively. ChIP was performed as described except using Mre11 polyclonal antibodies (49).

Purification of Recombinant Proteins and in Vitro Assays. The P110L mutation was generated in Mre11 expression vector pTP391 by site-directed mutagenesis, and the $Mre11^{P110L}$-Rad50-Xrs2 complex was purified from Sf9 cells as described (16). Yeast RPA was purified as described (16). DNA binding assays contained 25 mM TrisOAc (pH 7.5), 1 mM DTT, 5 mM $Mg(OAc)_2$ or 2 mM $MnCl_2$, 0 mM or 1 mM ATP, 250 μg/mL BSA with either 1 nM ssDNA (100 nt, 5′-end labeled) or dsDNA (100 base pairs dsDNA, 5′-end-labeled), and the indicated amount of MRX or $M^{P110L}RX$. Reactions were incubated at 30 °C for 10 min and then analyzed by electrophoresis using 5% (wt/vol) PAGE in 1× TAE at 4 °C. The gel was dried and quantified by using a Storm 860 PhosphorImager (GE Healthcare) with ImageQuant software. Nuclease assays were performed by using the same buffer except with 2 mM $MnCl_2$ or 5 mM Mg(OAc)2, 1 mM phosphoenolpyruvate and 80 units/mL pyruvate kinase, and with 2 nM (molecules) 3′ end-labeled dsDNA (50 bp). Reactions were incubated with 0.1 μM RPA and either 10 nM MRX or $M^{P110L}RX$ at 30 °C for the indicated time. Samples were analyzed by 15% (wt/vol) PAGE with 7.5 M urea in 1× TBE at 4 °C, and the dried gel was quantified with a Storm 860 PhosphorImager (GE Healthcare) by using ImageQuant software.

ACKNOWLEDGMENTS. We thank K. Lobachev, M. P. Longhese, T. Paull, T. Petes, and R. Rothstein for gifts of yeast strains and plasmids; M. Foiani for Rad53 antibodies; K. P. Hopfner for helpful discussion; Z. Zhou for assistance with microscopy; and F. Chang and R. Rothstein for use of their microscopes. This study was supported by National Institutes of Health Grants R01GM041784 (to L.S.S.), P01CA174653 (to L.S.S.), and R01GM062653 (to S.C.K.). R.A.D. was supported by an International Fellowship in Cancer Research cofunded by Italian Association for Cancer Research and Marie Curie Actions.

1. Harrison JC, Haber JE (2006) Surviving the breakup: The DNA damage checkpoint. *Annu Rev Genet* 40:209–235.
2. Gobbini E, Cesena D, Galbiati A, Lockhart A, Longhese MP (2013) Interplays between ATM/Tel1 and ATR/Mec1 in sensing and signaling DNA double-strand breaks. *DNA Repair (Amst)* 12(10):791–799.
3. Uziel T, et al. (2003) Requirement of the MRN complex for ATM activation by DNA damage. *EMBO J* 22(20):5612–5621.
4. Zou L, Elledge SJ (2003) Sensing DNA damage through ATRIP recognition of RPA-ssDNA complexes. *Science* 300(5625):1542–1548.
5. Stracker TH, Petrini JH (2011) The MRE11 complex: Starting from the ends. *Nat Rev Mol Cell Biol* 12(2):90–103.
6. Williams RS, et al. (2008) Mre11 dimers coordinate DNA end bridging and nuclease processing in double-strand-break repair. *Cell* 135(1):97–109.
7. Garcia V, Phelps SE, Gray S, Neale MJ (2011) Bidirectional resection of DNA double-strand breaks by Mre11 and Exo1. *Nature* 479(7372):241–244.
8. Neale MJ, Pan J, Keeney S (2005) Endonucleolytic processing of covalent protein-linked DNA double-strand breaks. *Nature* 436(7053):1053–1057.
9. Shibata A, et al. (2014) DNA double-strand break repair pathway choice is directed by distinct MRE11 nuclease activities. *Mol Cell* 53(1):7–18.
10. Zakharyevich K, et al. (2010) Temporally and biochemically distinct activities of Exo1 during meiosis: Double-strand break resection and resolution of double Holliday junctions. *Mol Cell* 40(6):1001–1015.

11. Cannavo E, Cejka P (2014) Sae2 promotes dsDNA endonuclease activity within Mre11-Rad50-Xrs2 to resect DNA breaks. *Nature* 514(7520):122–125.
12. Cejka P, et al. (2010) DNA end resection by Dna2-Sgs1-RPA and its stimulation by Top3-Rmi1 and Mre11-Rad50-Xrs2. *Nature* 467(7311):112–116.
13. Nimonkar AV, et al. (2011) BLM-DNA2-RPA-MRN and EXO1-BLM-RPA-MRN constitute two DNA end resection machineries for human DNA break repair. *Genes Dev* 25(4): 350–362.
14. Niu H, et al. (2010) Mechanism of the ATP-dependent DNA end-resection machinery from Saccharomyces cerevisiae. *Nature* 467(7311):108–111.
15. Shim EY, et al. (2010) Saccharomyces cerevisiae Mre11/Rad50/Xrs2 and Ku proteins regulate association of Exo1 and Dna2 with DNA breaks. *EMBO J* 29(19):3370–3380.
16. Cannavo E, Cejka P, Kowalczykowski SC (2013) Relationship of DNA degradation by Saccharomyces cerevisiae exonuclease 1 and its stimulation by RPA and Mre11-Rad50-Xrs2 to DNA end resection. *Proc Natl Acad Sci USA* 110(18):E1661–E1668.
17. Symington LS, Gautier J (2011) Double-strand break end resection and repair pathway choice. *Annu Rev Genet* 45:247–271.
18. Mimitou EP, Symington LS (2009) DNA end resection: Many nucleases make light work. *DNA Repair (Amst)* 8(9):983–995.
19. Lobachev KS, Gordenin DA, Resnick MA (2002) The Mre11 complex is required for repair of hairpin-capped double-strand breaks and prevention of chromosome rearrangements. *Cell* 108(2):183–193.
20. McKee AH, Kleckner N (1997) A general method for identifying recessive diploid-specific mutations in Saccharomyces cerevisiae, its application to the isolation of mutants blocked at intermediate stages of meiotic prophase and characterization of a new gene SAE2. *Genetics* 146(3):797–816.
21. Prinz S, Amon A, Klein F (1997) Isolation of COM1, a new gene required to complete meiotic double-strand break-induced recombination in Saccharomyces cerevisiae. *Genetics* 146(3):781–795.
22. Rattray AJ, McGill CB, Shafer BK, Strathern JN (2001) Fidelity of mitotic double-strand-break repair in Saccharomyces cerevisiae: A role for SAE2/COM1. *Genetics* 158(1):109–122.
23. Mimitou EP, Symington LS (2010) Ku prevents Exo1 and Sgs1-dependent resection of DNA ends in the absence of a functional MRX complex or Sae2. *EMBO J* 29(19):3358–3369.
24. Alani E, Padmore R, Kleckner N (1990) Analysis of wild-type and rad50 mutants of yeast suggests an intimate relationship between meiotic chromosome synapsis and recombination. *Cell* 61(3):419–436.
25. Clerici M, Mantiero D, Lucchini G, Longhese MP (2006) The Saccharomyces cerevisiae Sae2 protein negatively regulates DNA damage checkpoint signalling. *EMBO Rep* 7(2):212–218.
26. Lee SE, et al. (1998) Saccharomyces Ku70, mre11/rad50 and RPA proteins regulate adaptation to G2/M arrest after DNA damage. *Cell* 94(3):399–409.
27. Schiller CB, et al. (2012) Structure of Mre11-Nbs1 complex yields insights into ataxia-telangiectasia-like disease mutations and DNA damage signaling. *Nat Struct Mol Biol* 19(7):693–700.
28. Langerak P, Mejia-Ramirez E, Limbo O, Russell P (2011) Release of Ku and MRN from DNA ends by Mre11 nuclease activity and Ctp1 is required for homologous recombination repair of double-strand breaks. *PLoS Genet* 7(9):e1002271.
29. Clerici M, Mantiero D, Lucchini G, Longhese MP (2005) The Saccharomyces cerevisiae Sae2 protein promotes resection and bridging of double strand break ends. *J Biol Chem* 280(46):38631–38638.
30. Hardy J, Churikov D, Géli V, Simon MN (2014) Sgs1 and Sae2 promote telomere replication by limiting accumulation of ssDNA. *Nat Commun* 5:5004.
31. Usui T, Ogawa H, Petrini JH (2001) A DNA damage response pathway controlled by Tel1 and the Mre11 complex. *Mol Cell* 7(6):1255–1266.
32. Lisby M, Barlow JH, Burgess RC, Rothstein R (2004) Choreography of the DNA damage response: Spatiotemporal relationships among checkpoint and repair proteins. *Cell* 118(6):699–713.
33. Lee K, Lee SE (2007) Saccharomyces cerevisiae Sae2- and Tel1-dependent single-strand DNA formation at DNA break promotes microhomology-mediated end joining. *Genetics* 176(4):2003–2014.
34. Deng SK, Gibb B, de Almeida MJ, Greene EC, Symington LS (2014) RPA antagonizes microhomology-mediated repair of DNA double-strand breaks. *Nat Struct Mol Biol* 21(4):405–412.
35. Mimitou EP, Symington LS (2008) Sae2, Exo1 and Sgs1 collaborate in DNA double-strand break processing. *Nature* 455(7214):770–774.
36. Gravel S, Chapman JR, Magill C, Jackson SP (2008) DNA helicases Sgs1 and BLM promote DNA double-strand break resection. *Genes Dev* 22(20):2767–2772.
37. Zhu Z, Chung WH, Shim EY, Lee SE, Ira G (2008) Sgs1 helicase and two nucleases Dna2 and Exo1 resect DNA double-strand break ends. *Cell* 134(6):981–994.
38. Foster SS, Balestrini A, Petrini JH (2011) Functional interplay of the Mre11 nuclease and Ku in the response to replication-associated DNA damage. *Mol Cell Biol* 31(21): 4379–4389.
39. Limbo O, et al. (2007) Ctp1 is a cell-cycle-regulated protein that functions with Mre11 complex to control double-strand break repair by homologous recombination. *Mol Cell* 28(1):134–146.
40. Bonetti D, et al. (2015) Escape of Sgs1 from Rad9 inhibition reduces the requirement for Sae2 and functional MRX in DNA end resection. *EMBO Rep* 16(3):351–360.
41. Ferrari M, et al. (2015) Functional interplay between the 53BP1-ortholog Rad9 and the Mre11 complex regulates resection, end-tethering and repair of a double-strand break. *PLoS Genet* 11(1):e1004928.
42. Sun Z, Fay DS, Marini F, Foiani M, Stern DF (1996) Spk1/Rad53 is regulated by Mec1-dependent protein phosphorylation in DNA replication and damage checkpoint pathways. *Genes Dev* 10(4):395–406.
43. Sanchez Y, et al. (1996) Regulation of RAD53 by the ATM-like kinases MEC1 and TEL1 in yeast cell cycle checkpoint pathways. *Science* 271(5247):357–360.
44. Limbo O, Porter-Goff ME, Rhind N, Russell P (2011) Mre11 nuclease activity and Ctp1 regulate Chk1 activation by Rad3ATR and Tel1ATM checkpoint kinases at double-strand breaks. *Mol Cell Biol* 31(3):573–583.
45. Bernstein KA, et al. (2013) Resection activity of the Sgs1 helicase alters the affinity of DNA ends for homologous recombination proteins in Saccharomyces cerevisiae. *Genetics* 195(4):1241–1251.
46. Lengsfeld BM, Rattray AJ, Bhaskara V, Ghirlando R, Paull TT (2007) Sae2 is an endonuclease that processes hairpin DNA cooperatively with the Mre11/Rad50/Xrs2 complex. *Mol Cell* 28(4):638–651.
47. Amberg DC, Burke DJ, Strathern JN (2005) *Methods in Yeast Genetics: A Cold Spring Harbor Laboratory Course Manual* (Cold Spring Harbor Lab Press, Plainview, NY).
48. Krogh BO, Llorente B, Lam A, Symington LS (2005) Mutations in Mre11 phosphoesterase motif I that impair Saccharomyces cerevisiae Mre11-Rad50-Xrs2 complex stability in addition to nuclease activity. *Genetics* 171(4):1561–1570.
49. Donnianni RA, et al. (2010) Elevated levels of the polo kinase Cdc5 override the Mec1/ATR checkpoint in budding yeast by acting at different steps of the signaling pathway. *PLoS Genet* 6(1):e1000763.